PERGAMON

Chemical Engineering Science 56 (2001) 537–545

Chemical Engineering Science

www.elsevier.nl/locate/ces

Design and scale up of a bubble column slurry reactor for Fischer–Tropsch synthesis

R. Krishna*, J. M. van Baten, M. I. Urseanu, J. Ellenberger

Department of Chemical Engineering, University of Amsterdam, Nieuwe Achtergracht 166, 1018 WV Amsterdam, Netherlands

Abstract

We develop a strategy for scaling up a bubble column slurry reactor, which is used for example for carrying out the Fischer–Tropsch synthesis reaction. The strategy involves development of a proper description for the large bubble swarm velocity in highly concentrated paraffin-oil slurries in columns of varying diameters. The developed relationship is incorporated into an Eulerian simulation code which is then used to predict the hydrodynamic parameters (hold-up, velocity distribution, etc.) for reactors of commercial scale. © 2001 Elsevier Science Ltd. All rights reserved.

Keywords: Bubble columns; Churn-turbulent flow regime; Bubble rise velocity; Radial velocity profiles; Column diameter influence; Axial dispersion coefficient

1. Introduction

There is considerable industrial interest in the design and scale-up of the bubble column slurry reactor for Fischer–Tropsch synthesis of heavy paraffins starting with syngas ($CO + H_2$) (Krishna & Sie, 2000; Maretto & Krishna, 1999; Sie & Krishna, 1999). There are several aspects of this reactor that make the scale-up task particularly daunting.

1. Large gas throughputs are involved, necessitating the use of large diameter reactors, typically 6–8 m.
2. The process operates under high-pressure conditions, typically 3–4 MPa.
3. In order to achieve gas conversions in excess of 90%, tall reactors, typically 30–40 m, are required.
4. To achieve high reactor productivities highly concentrated slurries, approaching 40 vol%, need to be used, and
5. The process is highly exothermic in nature, requiring heat removal by means of cooling tubes inserted in the reactor.

Most of these process conditions fall outside the purview of most literature data and correlations (Deckwer, 1992; Krishna, 2000; Wilkinson, Spek & van Dierendonck, 1992).

The major objective of this communication is to develop a systematic design and scale-up procedure for the Fischer–Tropsch bubble column slurry reactor. The strategy relies on experimental data with a variety of liquids and paraffin-oil slurries of varying concentrations in columns of varying diameter. The developed insights into the hydrodynamics are incorporated into an Eulerian simulation code for scaling up to reactors of commercial size.

2. Experimental

Experiments were performed in polyacrylate columns with inner diameters of 0.1, 0.19 and 0.38 m. The gas distributors used in the three columns were all made of sintered bronze plate (with a mean pore size of 50 μm). All columns were equipped with quick closing valves in the gas inlet pipe in order to perform dynamic gas disengagement, or bed collapse experiments. Air was used as the gas phase in all experiments. Experiments were performed with paraffin-oil (density, $\rho_L = 790\ \mathrm{kg/m^3}$; viscosity, $\mu_L = 0.0029$ Pa s; surface tension, $\sigma = 0.028$ N/m) as liquid phase to which solid particles in varying concentrations were added. The solid phase used consisted of porous silica particles whose properties were determined to be as follows: skeleton density $= 2100\ \mathrm{kg/m^3}$; pore

* Corresponding author. Tel.: + 31-20-525-7007; fax: + 31-20-525-5604.

E-mail address: krishna@its.chem.uva.nl (R. Krishna).

0009-2509/01/$ - see front matter
PII: S0009-2509(00)00258-X

volume = 1.05 ml/g; particle size distribution, d_p: 10% < 27 μm; 50% < 38 μm; 90% < 47 μm. The solids concentration ε_s, is expressed as the volume fraction of solids in gas-free slurry. The pore volume of the particles (liquid filled during operation) is counted as being part of the solid phase. To investigate the gas hold-up characteristics in the churn-turbulent regime, dynamic gas disengagement experiments were performed. Analogous experiments to determine the total gas hold-up and distribution of hold-ups of the "large" and "small" bubbles were also carried out with Tellus oil ($\rho_L = 862$; $\mu_L = 0.075$; $\sigma = 0.028$) and demineralised water ($\rho_L = 998$; $\mu_L = 0.001$; $\sigma = 0.072$) as the liquid phase.

The axial component of the liquid velocities along the radial positions at different superficial gas velocities were measured using a modified Pitot tube, also called "Pavlov tube" (for details of the measurement technique, see Hills (1974) and Krishna, Urseanu, van Baten & Ellenberger (1999b)), in three columns with different inner diameters: 0.174, 0.38 and 0.63 m with the air–water system and in the 0.38 m diameter column with Tellus oil. All three columns were made up of four polyacrylate sections with the total height of 4 m. In all three columns the pressure at the top corresponded to ambient conditions (101.3 kPa). The 0.63 m column was provided with a spider-shaped sparger, described in earlier work (Krishna & Ellenberger, 1996).

3. Gas hold-up

The influence of the solids concentration on the total gas hold-up ε for varying superficial gas velocities U is shown in Fig. 1(a) for the 0.10 m diameter column. It is observed that increased particles concentration tends to decrease ε to a significant extent. This decrease in ε is due to the reduction in the hold-up of the small bubbles, ε_{df}, from enhanced coalescence caused by the presence of the catalyst particles. Typical dynamic gas disengagement profiles for air–paraffin oil and air – 36 vol% paraffin oil slurry in the 0.38 m column for $U = 0.25$ m/s are shown in Fig. 2(a). After the shut-off of the gas supply, the hold-up decreases due to the escape of fast rising "large" bubbles ("dilute" phase). When the "large" bubbles have escaped the "small" bubbles leave the column. The terminology of "dilute" and "dense" phases is based on the "two-phase" model adopted earlier to describe the hydrodynamics of bubble columns in the churn-turbulent flow regime (Krishna & Ellenberger, 1996; Krishna, de Swart, Ellenberger, Martina & Maretto, 1997; Krishna, Urseanu, de Swart & Ellenberger, 2000) (see Fig. 3). For the air–paraffin oil system the small bubbles are typically in the 1–4 mm size range and the large bubbles are in the 15–50 mm size range; these two bubble classes have different rise characteristics (Krishna & van Baten, 1999). The "dense" phase is identified with the liquid phase along with the catalyst particles and the entrained "small" bubbles.

Fig. 1(b) shows the collection of data on the gas hold-up in the dense-phase, ε_{df}, for all column diameters and slurry concentrations; this corresponds to the hold-up of the small bubbles in the dense phase. We see that the dense phase gas hold-up ε_{df} is virtually independent of the column diameter and is a significant decreasing function of the particle concentration ε_s. The unique dependence of the decrease in the dense-phase gas voidage ε_{df} with increasing solids volume fraction ε_s is useful for scale-up purposes because this parameter can be determined in a relatively small diameter column under actual reaction conditions of temperature and pressure. It is clear that addition of silica particles has the effect of reducing the small bubble population virtually to zero when the slurry concentration approaches 40 vol%. The addition of catalyst particles tends to promote coalescence of small bubbles and so the rise velocity of the small bubbles, V_{small}, increases with increasing ε_s. The

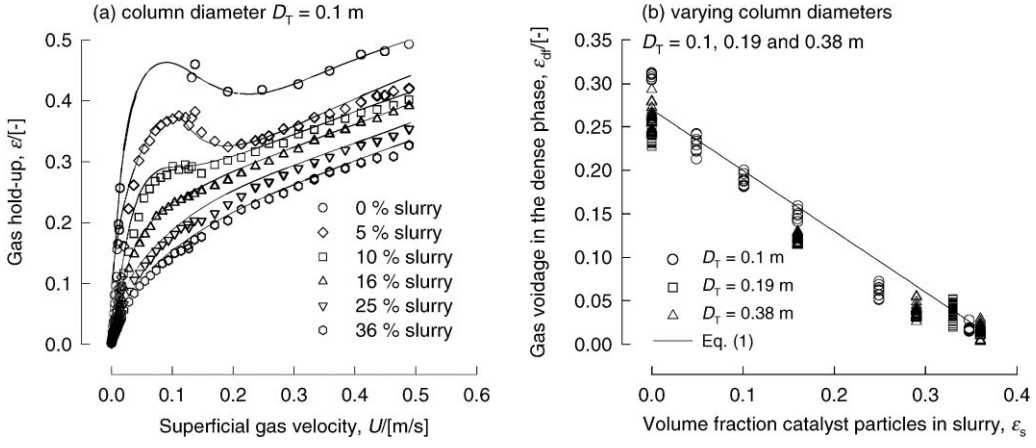

Fig. 1. (a) Influence of increased particles concentration on the total gas hold-up in 0.1 m diameter column. (b) Influence of particles concentration ε_s. on dense-phase gas voidage, ε_{df}.

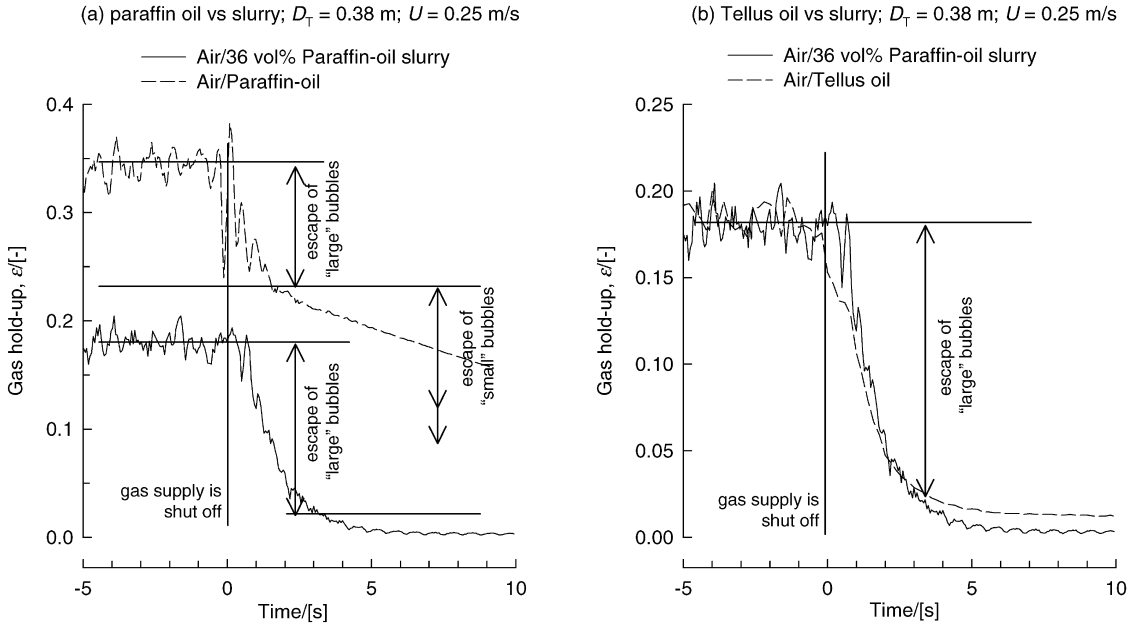

Fig. 2. (a) Dynamic gas disengagement experiments for air/paraffin oil and air/36 vol% paraffin oil slurry in the 0.38 m diameter column. (b) Comparison of DGD for 36 vol% paraffin slurry and air–Tellus oil.

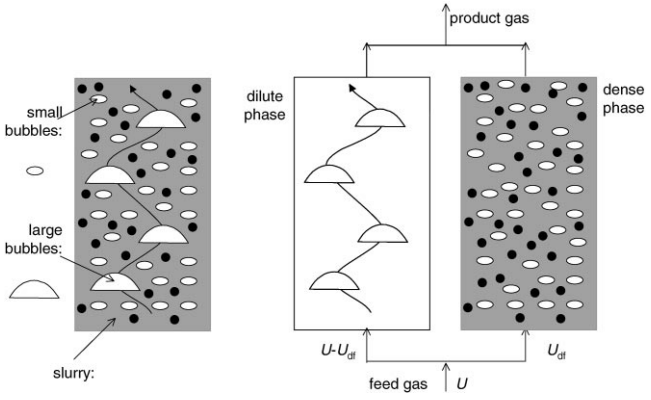

Fig. 3. Two-phase model for slurry reactor.

paraffin–oil slurry data on ε_{df} and V_{small}, can be correlated as follows:

$$\varepsilon_{df} = \varepsilon_{df,0}\left(1 - \frac{0.7}{\varepsilon_{df,0}}\varepsilon_s\right), \tag{1}$$

$$V_{\text{small}} = V_{\text{small},0}\left(1 + \frac{0.8}{V_{\text{small},0}}\varepsilon_s\right). \tag{2}$$

The paraffin–oil parameters (corresponding to $\varepsilon_s = 0$) are $\varepsilon_{df,0} = 0.27$ and $V_{\text{small},0} = 0.095$ m/s. The superficial gas velocity through the dense phase can be estimated from

$$U_{df} = V_{\text{small}}\varepsilon_{df}. \tag{3}$$

Our earlier study on the modelling of the Fischer–Tropsch slurry reactor has shown that slurry concentration of at least 35 vol% is desirable from the point of view of commercial viability (Maretto & Krishna, 1999). We, therefore, focus further attention on the influence of column diameter on the hydrodynamics of a 36 vol% paraffin oil slurry system. The total gas hold-up ε measured with this slurry concentration in the three columns are compared in Fig. 4 with the corresponding data obtained with air–Tellus oil. It is interesting to note that the gas hold-ups for Tellus oil and slurry systems are remarkably close to each another for all three columns studied.

Dynamic gas disengagement experiments were also performed in the three columns with air–Tellus oil. A typical experiment carried out in the 0.38 m diameter column operating at a superficial gas velocity $U = 0.25$ m/s is shown in Fig. 2(b), in which comparison is made with the corresponding experiment with the air – 36 vol% slurry. In the air–Tellus oil system, the dispersion consists predominantly of large bubbles and the values of the dense-phase voidage $\varepsilon_{df} \approx 0.02$ and $U_{df} \approx 0.01$ m/s.

From the dynamic gas disengagement experiments, the large bubble swarm velocity was determined for both air–Tellus oil and air–paraffin oil slurries. The experimental data are shown in Figs. 5(a) and (b) for the respective systems. The large bubble rise velocity V_b increases significantly with increasing column diameter. The continuous lines drawn in Fig. 5 represent calculations of the model developed by Krishna, Urseanu, van Baten and Ellenberger (1999a). In this model we introduce two correction factors into the classical Davies–Taylor relation for the rise of a single spherical cap bubble in an infinite volume of liquid.

$$V_b = 0.71\sqrt{gd_b}(\text{SF})(\text{AF}). \tag{4}$$

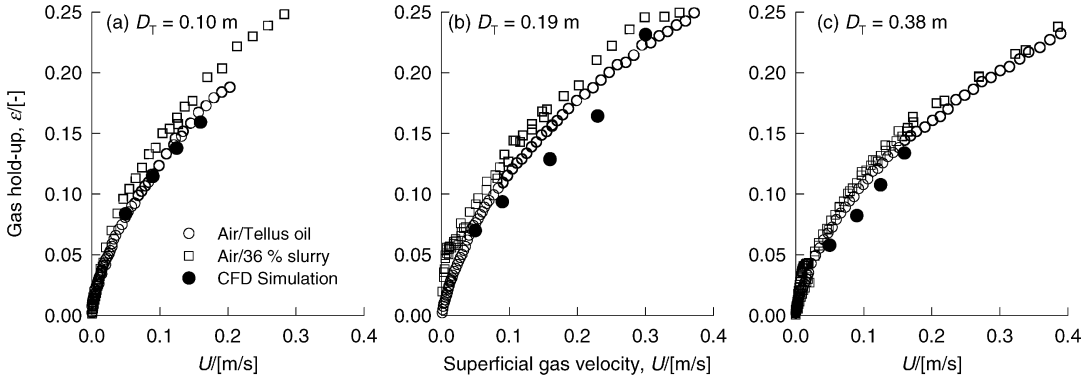

Fig. 4. Comparison of gas hold-up in Tellus oil and concentrated paraffin-oil slurries in columns of 0.1, 0.19 and 0.38 m diameter. Also shown are Eulerian simulations of the large bubble hold-up in air–Tellus oil system.

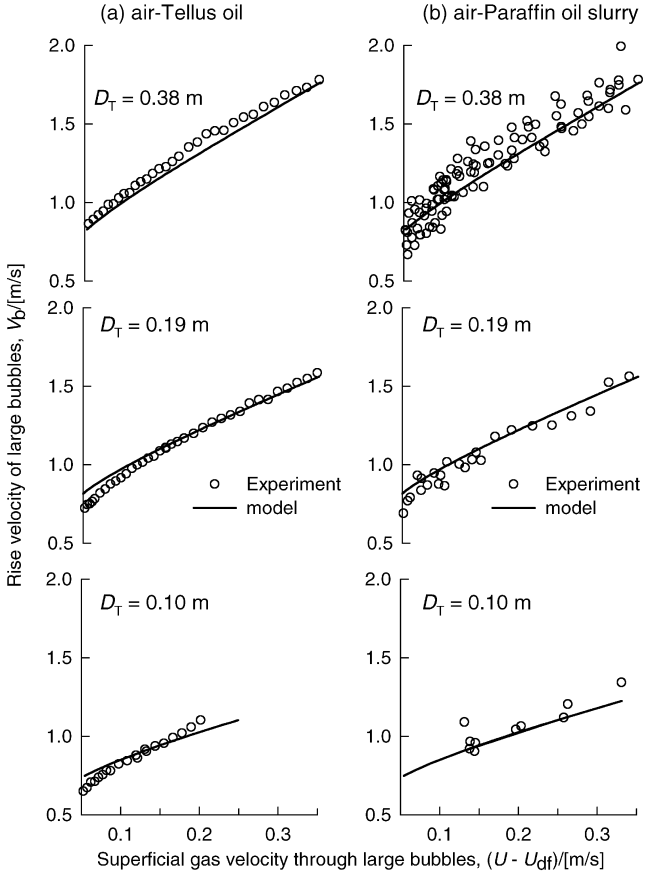

Fig. 5. Large bubble rise velocity in air–Tellus oil (left) and in concentrated paraffin oil slurries (right). Data measured in columns of three different diameters, 0.1, 0.19 and 0.38 m compared with model Eqs. (1)–(8).

The scale correction factor SF accounts for the influence of the column diameter and is taken from the work of Collins (1967) to be a function of the ratio of the bubble diameter d_b to the column diameter, D_T:

$$\mathrm{SF} = \begin{cases} 1 & \text{for } d_b/D_T < 0.125, \\ 1.13\exp(-d_b/D_T) & \text{for } 0.125 < d_b/D_T < 0.6, \\ 0.496\sqrt{D_T/d_b} & \text{for } d_b/D_T > 0.6. \end{cases} \quad (5)$$

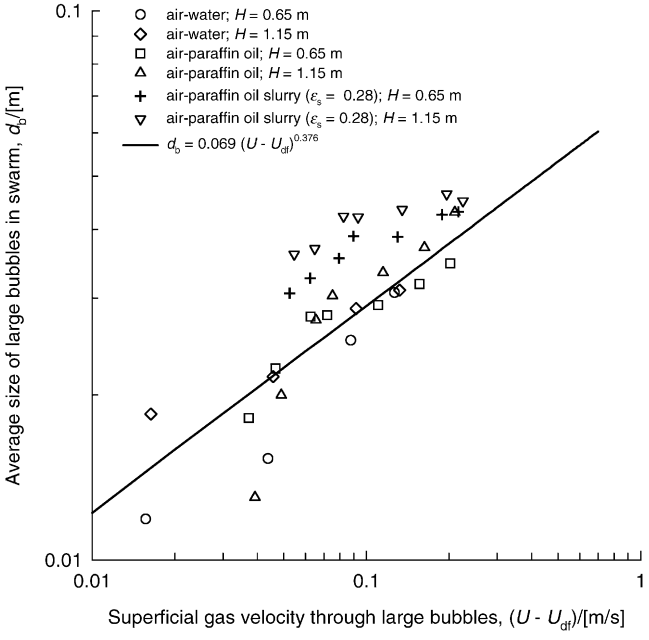

Fig. 6. Large bubble size in water, paraffin-oil and paraffin-oil slurries as a function of $(U - U_{df})$.

The acceleration factor AF accounts for the increase in the large bubble rise velocity over that of a single, isolated, bubble; this acceleration is due to wake interactions. This factor increases as the distance between the large bubbles decreases. For air–Tellus oil the following correlation has been developed:

$$\mathrm{AF} = 2.25 + 4.09(U - U_{df}). \quad (6)$$

The average large bubble size in the swarm can be estimated from the following empirical relationship:

$$d_b = 0.069(U - U_{df})^{0.376}. \quad (7)$$

Eq. (7) is in reasonable agreement with measured experimental data of de Swart, van Vliet and Krishna (1996) in a rectangular two-dimensional column with air–water and air–paraffin oil slurries (see Fig. 6).

The total gas hold-up can be calculated from

$$\varepsilon = \varepsilon_b + \varepsilon_{df}(1 - \varepsilon_b). \tag{8}$$

The predictions of the model represented by Eqs. (1)–(7) agree very well with the experimental data for V_b for both air–Tellus oil and air – 36% slurry systems (see Figs. 5(a) and (b)).

The phenomenological model given by Eqs. (1)–(7) to describe the bubble diameter, rise velocity and hold-ups will now be incorporated into a more fundamental model for scale-up relying on computational fluid dynamics (CFD) in the Eulerian framework.

4. Eulerian simulation model for bubble column slurry reactor

For scale-up purposes we adopt the two-phase model shown in Fig. 3. In the heterogeneous flow regime, the small bubbles have the backmixing characteristics of the liquid, or slurry, phase. For slurries with concentration higher than 36 vol%, the small bubble hold-up is virtually destroyed and so we take $U_{df} \approx 0$. We develop an Eulerian simulation model for the situation with concentrated slurries, and model the slurry phase as a pseudo-liquid phase with properties of Tellus oil. For either the large bubble or liquid phase, the volume-averaged mass and momentum conservation equations in the Eulerian framework are given by

$$\frac{\partial(\varepsilon_k \rho_k)}{\partial t} + \nabla\bullet(\rho_k \varepsilon_k \mathbf{u}_k) = 0, \tag{9}$$

$$\frac{\partial(\rho_k \varepsilon_k \mathbf{u}_k)}{\partial t} + \nabla\bullet(\rho_k \varepsilon_k \mathbf{u}_k \mathbf{u}_k - \mu_k \varepsilon_k(\nabla \mathbf{u}_k + (\nabla \mathbf{u}_k)^{\mathrm{T}})) = -\varepsilon_k \nabla p + \mathbf{M}_{kl} + \rho_k \mathbf{g}. \tag{10}$$

The momentum exchange between the large bubble and liquid phase is given by

$$\mathbf{M}_{L,b} = \frac{3}{4}\rho_L \frac{\varepsilon_b}{d_b} C_D(\mathbf{u}_b - \mathbf{u}_L)|\mathbf{u}_b - \mathbf{u}_L|, \tag{11}$$

where the drag coefficient, defined by

$$C_D = \frac{4}{3}\frac{\rho_L - \rho_G}{\rho_L} g d_b \frac{1}{V_b^2} \tag{12}$$

can be estimated by inserting Eq. (4) for the large bubble rise velocity V_b. We have only included the drag force contribution to $\mathbf{M}_{L,b}$, in keeping with the works of Sanyal, Vasquez, Roy and Dudukovic (1999) and Sokolichin and Eigenberger (1999). The added mass force has been ignored in the present analysis because large bubbles do not have a closed wake and the concept of added mass is not applicable. Lift forces are also ignored in the present analysis because of the uncertainty in assigning values of the lift coefficients to large bubbles (Jakobsen, Sannæs, Grevskott & Svendsen, 1997). For the continuous, liquid, phase, the turbulent contribution to the stress tensor is evaluated by means of k–ε model, using standard single-phase parameters:

$$C_\mu = 0.09, \qquad C_{1\varepsilon} = 1.44, \qquad C_{2\varepsilon} = 1.92, \qquad \sigma_k = 1, \qquad \sigma_\varepsilon = 1.3. \tag{13}$$

The applicability of the k–ε model has been considered in detail by Sokolichin and Eigenberger (1999). No turbulence model is used for calculating the velocity fields inside the dispersed "large" bubble phase.

A commercial CFD package CFX 4.2 of AEA Technology, Harwell, UK, was used to solve the equations of continuity and momentum. This package is a finite volume solver, using body-fitted grids. The grids are non-staggered and all variables are evaluated at the cell centres. An improved version of the Rhie–Chow algorithm is used to calculate the velocity at the cell faces. The pressure–velocity coupling is obtained using the SIMPLEC algorithm. For the convective terms in Eqs. (9) and (10) hybrid differencing was used. A fully implicit backward differencing scheme was used for the time integration. Further details of the implementation of the Eulerian simulation code are available in our earlier publications (Krishna, Urseanu, van Baten & Ellenberger, 1999b, 2000; Krishna, van Baten & Urseanu, 2000).

Simulations were carried out for a variety of column diameters and superficial gas velocities as specified in Table 1. In all simulations the aspect ratio was chosen to be at least 5. The large bubbles were injected in the central core of the column because this is in conformity with visual observations. The simulations were carried out using cylindrical axisymmetry. The time-stepping strategy used in the transient simulations for attainment of steady state was typically: 20 steps at 5×10^{-4} s, 20 steps at 1×10^{-3} s, 460 steps at 5×10^{-3} s, 2000 steps at 2×10^{-2} s. The 0.1, 0.19 and 0.38 m diameter column simulations were carried out on a Silicon Graphics Power Indigo workstation with the R8000 processor. Each simulation was completed in about 36 h. In all the runs steady state was reached within 2500 time steps. Simulations of the 1.5, 2, 4 and 6 m diameter columns were carried out on a Silicon Graphics Power Challenge machine employing three R10000 processors in parallel. In order to check for grid independence, we ran the 2 m column diameter simulation ($U = 0.16$ m/s) with both coarse (75×270 cells) and fine grid (75×780 cells). The results were in agreement to within 2%. Further

Table 1
Column configurations, operating conditions and grid details of 2D axisymmetric Eulerian simulations for air–Tellus oil system. The large bubble phase was injected over the central 13 (or 32) of the 30 (or 75) grid cells

Column diameter D_T (m)	Column height (m)	Initial liquid height (m)	No. of grid cells (radial) × (axial)	Superficial gas velocity, U (m/s)
0.1	2	1.4	30 × 110	0.05, 0.09, 0.125, 0.16
0.19	2	1.4	30 × 110	0.05, 0.09, 0.16, 0.23, 0.3, 0.35
0.38	2	1.4	30 × 110	0.05, 0.09, 0.125, 0.16, 0.23, 0.3, 0.35
1.5	8	5.3	75 × 410	0.05, 0.09, 0.16
2	13	10	75 × 270	0.16, 0.3
2	13	10	75 × 780 (Fine grid)	0.16
4	25	20	75 × 510	0.16, 0.3
6	35	20	75 × 710	0.16, 0.3

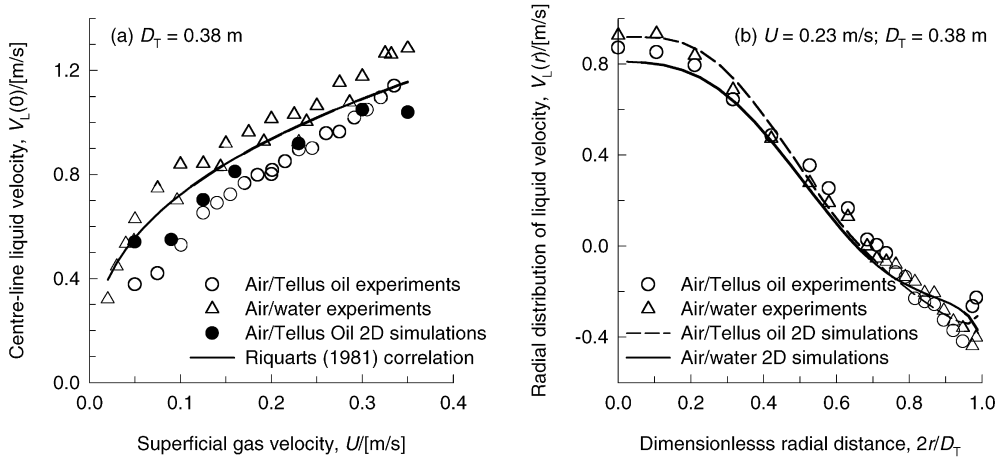

Fig. 7. Comparison of experimental (a) centreline velocity data $V_L(0)$ and (b) radial distribution $V_L(r)$ for air–water and air–Tellus oil systems in 0.38 m diameter column with Eulerian simulations of air–Tellus oil.

details of simulations, including animations of column start-up dynamics are available on our web site: http://ct-cr4.chem.uva.nl/oil-water.

The total gas hold-up determined from Eulerian simulations for the three column diameters are also shown in Fig. 4. The agreement with the measurements with concentrated slurry and Tellus oil is reasonably good. The measured centreline velocities $V_L(0)$ and radial distribution $V_L(r)$ for the air–Tellus oil system in the 0.38 m diameter column are compared in Fig. 7 with Eulerian simulations and experimental data for water. Two conclusions emerge: (a) the agreement between Eulerian simulations and experiments is good, and (b) as regards the liquid velocity profiles are concerned there is no difference between a highly viscous liquid and a low viscosity liquid such as water. The centreline velocity $V_L(0)$ data in Fig. 7(a) are adequately represented by the correlation of Riquarts (1981):

$$V_L(0) = 0.21(gD_T)^{1/2}(U^3/gv_L)^{1/8} \quad (14)$$

provided the water properties are used, i.e. $v_L = 10^{-6}$ m^2/s.

The Eulerian simulation results for the large bubble hold-up and the centreline liquid velocity with increasing column diameter to 6 m are shown in Fig. 8. Our Eulerian simulations show a strong increase in $V_L(0)$ with increasing D_T. This increase with scale follows the square-root dependence on column diameter as given by the Riquarts correlation (14). This strong increase in the liquid circulations with increasing scale leads to a significant reduction in the hold-up of the large bubbles. This decrease in the large bubble hold-up is not anticipated by

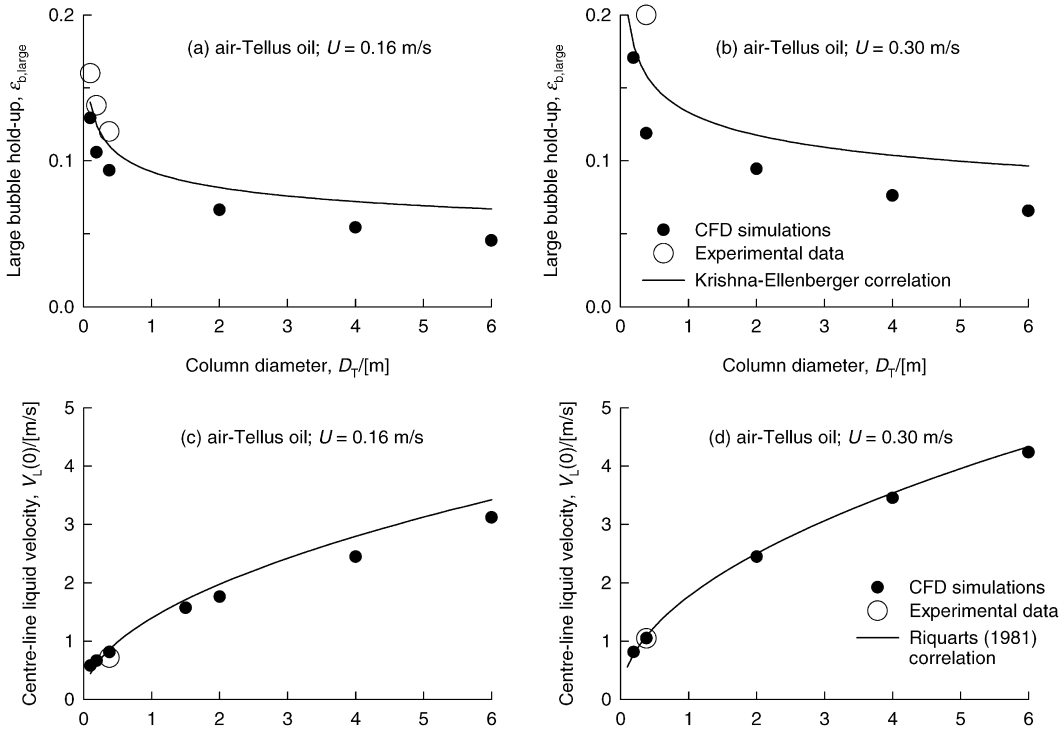

Fig. 8. Influence of scale on the hold-up of large bubbles and on the centreline liquid velocity. Predictions of 2D axisymmetric Eulerian simulations. Also shown is the Riquarts (1981) correlation for $V_L(0)$ and the Krishna and Ellenberger (1996) correlation for ε_b.

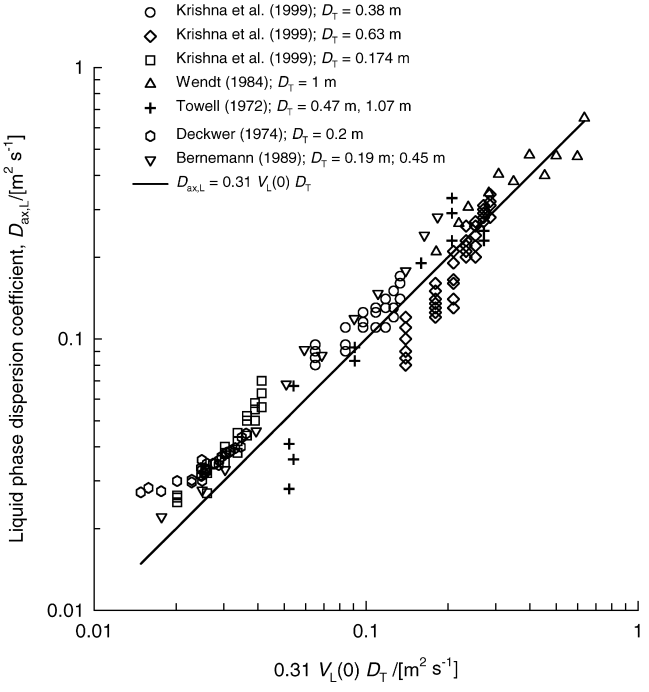

Fig. 9. Axial dispersion coefficient of the liquid phase. Experimental data from the literature compared with predictions using Eq. (15).

any of the published correlations (Krishna & Ellenberger, 1996; Wilkinson, Spek & van Dierendonck, 1992).

In order to predict the liquid phase backmixing as a function of scale, we recommend our previously developed correlation:

$$D_{\mathrm{ax},L} = 0.31 V_L(0) D_T, \tag{15}$$

wherein the $V_L(0)$ is calculated using Eq. (14) with water properties. Fig. 9 compares this prediction method with literature data on $D_{\mathrm{ax},L}$; the agreement with experimental data is very good for a wide range of column diameters.

5. Concluding remarks

We have demonstrated that the hydrodynamics of concentrated paraffin-oil slurries is equivalent to that of a highly viscous oil, such as Tellus oil. The model of Krishna et al. (1999a) for calculating the large bubble swarm velocity of Tellus oil works very well for paraffin-oil oil slurries. The Eulerian simulation model developed in this work provides a valuable tool for predicting the hydrodynamics of commercial-scale reactors. The simulations show a strong reduction in the large bubble hold-up with increasing column diameter due to strong increase in liquid circulations, characterised by $V_L(0)$. Our Eulerian simulations of columns with diameters

approaching 6 m confirms the validity of the Riquarts correlation (14) for scale-up purposes provided the properties of water are used. The liquid-phase backmixing coefficient $D_{ax,L}$ is simply proportional to the product of $V_L(0)$ and the column diameter D_T and can be predicted using Eq. (15).

Notation

AF	acceleration factor, dimensionless
d_b	diameter of either bubble population, m
C_D	drag coefficient, dimensionless
$D_{ax,L}$	liquid-phase axial dispersion coefficient, m^2/s
D_T	column diameter, m
g	acceleration due to gravity, 9.81 m/s^2
M	interphase momentum exchange term, N/m^3
p	pressure, N/m^2
r	radial coordinate, m
SF	scale correction factor, dimensionless
t	time, s
u	velocity vector, m/s
U	superficial gas velocity, m/s
V_b	rise velocity of bubble population, m/s
$V_L(r)$	radial distribution of liquid velocity, m/s
$V_L(0)$	centreline liquid velocity, m/s

Greek letters

ε	volume fraction of gas phase, dimensionless
μ	viscosity of phase, Pa s
ρ	density of phases, kg/m^3
σ	surface tension of liquid phase, N/m

Subscripts

0	referring to "pure" liquid (no catalyst)
b	referring to large bubble population
df	referring to the dense phase
G	referring to gas phase
k	index referring to either gas or liquid phase
L	referring to liquid phase
s	referring to solid catalyst particles
small	referring to small bubbles

Acknowledgements

Financial assistance from The Netherlands Organization for Scientific Research (NWO) in the form of a "programmasubsidie" to RK is gratefully acknowledged. JMvB is also grateful to NWO for grant of a Ph.D. fellowship.

References

Bernemann, K. (1989). *Zur Fluiddynamik und zum Vermischungsverhalten der flüssigen Phase in Blasensäulen mit längsangeströmten Rohrbundeln.* Ph.D. thesis, University of Dortmund.

Collins, R. (1967). The effect of a containing cylindrical boundary on the velocity of a large gas bubble in a liquid. *Journal of Fluid Mechanics*, *28*, 97–112.

Deckwer, W. D. (1992). *Bubble column reactors*. New York: Wiley.

Deckwer, W. D., Burckhart, R., & Zoll, G. (1974). Mixing and mass transfer in tall bubble columns. *Chemical Engineering Science*, *29*, 2177–2188.

Hills, J. H. (1974). Radial non-uniformity of velocity and voidage in a bubble column. *Transactions of the Institution of Chemical Engineers*, *52*, 1–9.

Jakobsen, H. A., Sannæs, B. H., Grevskott, S., & Svendsen, H. F. (1997). Modeling of bubble driven vertical flows. *Industrial and Engineering Chemistry Research*, *36*, 4052–4074.

Krishna, R. (2000). A scale-up strategy for a commercial scale bubble column slurry reactor for Fischer Tropsch synthesis. *Oil and Gas Science and Technology, Revue de L'Institut Francais du Petrole*, *55*, 359–393.

Krishna, R., & Ellenberger, J. (1996). Gas hold-up in bubble column reactors operating in the churn-turbulent flow regime. *American Institute of Chemical Engineers Journal*, *42*, 2627–2634.

Krishna, R., de Swart, J. W. A., Ellenberger, J., Martina, G. B., & Maretto, C. (1997). Gas holdup in slurry bubble columns. *American Institute of Chemical Engineers Journal*, *43*, 311–316.

Krishna, R., & Sie, S. T. (2000). Selection, design and scale-up aspects of Fischer–Tropsch reactors. *Fuel Processing Technology*, *64*, 73–105.

Krishna, R., Urseanu, M. I., de Swart, J. W. A., & Ellenberger, J. (2000). Gas hold-up in bubble columns: Operation with concentrated slurries versus high viscosity liquid. *Canadian Journal of Chemical Engineering*, *78*, 442–448.

Krishna, R., Urseanu, M. I., van Baten, J. M., & Ellenberger, J. (1999a). Rise velocity of a swarm of large gas bubbles in liquids. *Chemical Engineering Science*, *54*, 171–183.

Krishna, R., Urseanu, M. I., van Baten, J. M., & Ellenberger, J. (1999b). Influence of scale on the hydrodynamics of bubble columns operating in the churn-turbulent regime: Experiments vs. Eulerian simulations. *Chemical Engineering Science*, *54*, 4903–4911.

Krishna, R., Urseanu, M. I., van Baten, J. M., & Ellenberger, J. (2000). Liquid phase dispersion in bubble columns operating in the churn-turbulent flow regime. *Chemical Engineering Journal*, *78*, 43–51.

Krishna, R., & van Baten, J. M. (1999). Simulating the motion of gas bubbles in a liquid. *Nature*, *398*, 208.

Krishna, R., van Baten, J. M., & Urseanu, M. I. (2000). Three-phase Eulerian simulations of bubble column reactors operating in the churn-turbulent flow regime: A scale-up strategy. *Chemical Engineering Science*, *55*, 3275–3286.

Maretto, C., & Krishna, R. (1999). Modelling of a bubble column slurry reactor for Fischer–Tropsch synthesis. *Catalysis Today*, *52*, 279–289.

Riquarts, H. P. (1981). Strömungsprofile, Impulsaustausch und Durchmischung der flüssigen Phase in Bläsensaulen. *Chemie Ingenieur Technik*, *53*, 60–61.

Sanyal, J., Vasquez, S., Roy, S., & Dudukovic, M. P. (1999). Numerical simulation of gas–liquid dynamics in cylindrical bubble column reactors. *Chemical Engineering Science*, *54*, 5071–5083.

Sie, S. T., & Krishna, R. (1999). Fundamentals and selection of advanced Fischer–Tropsch reactors. *Applied Catalysis A*, *186*, 55–70.

Sokolichin, A., & Eigenberger, G. (1999). Applicability of the standard — turbulence model to the dynamic simulation of bubble columns:

Part I. Detailed numerical simulations. *Chemical Engineering Science*, *54*, 2273–2284.

de Swart, J. W. A., van Vliet, R. E., & Krishna, R. (1996). Size, structure and dynamics of "large" bubbles in a 2-D slurry bubble column. *Chemical Engineering Science*, *51*, 4619–4629.

Towell, G. D., & Ackerman, G. H. (1972). Axial mixing of liquids and gas in large bubble reactor. *Proceedings of the second international symposium on chemical reaction engineering*, Amsterdam, The Netherlands (pp. B3.1–B3.13).

Wendt, R., Steiff, A., & Weinspach, P. M. (1984). Liquid phase dispersion in bubble columns. *German Chemical Engineering*, *7*, 267–273.

Wilkinson, P. M., Spek, A. P., & van Dierendonck, L. L. (1992). Design parameters estimation for scale-up of high-pressure bubble columns. *American Institute of Chemical Engineers Journal*, *38*, 544–554.